

2225 Rpnud

# Stress Relaxation in Short Sisal-Fiber-Reinforced Natural Rubber Composites

SIBY VARGHESE,<sup>1</sup> BABY KURIAKOSE,<sup>1,\*</sup> and SABU THOMAS<sup>2</sup>

<sup>1</sup>Rubber Research Institute of India, Kottayam—686 009, Kerala, India, and <sup>2</sup>School of Chemical Sciences, Mahatma Gandhi University, Priyadarshini Hills P.O., Kottayam—686 560, Kerala, India

## SYNOPSIS

Stress relaxation behavior of chemically treated short sisal fiber-reinforced natural rubber composite was studied. The effect of bonding agent, strain level, fiber loading, fiber orientation, and temperature has been studied in detail. The existence of a single relaxation pattern in the unfilled stock and a two-stage relaxation mechanism for the fiber-filled composite is reported. The relaxation process is influenced by the bonding agent, which indicated that the process involved fiber-rubber interface. The rate of stress relaxation increased with fiber loading, whereas it decreased with aging. © 1994 John Wiley & Sons, Inc.

## INTRODUCTION

Recently short fiber-reinforced elastomers have gained wide importance due to the advantages in processing and low cost coupled with high strength. The properties of the composites depend on fiber concentration, fiber dispersion, fiber-matrix adhesion, fiber orientation, and aspect ratio of fiber. Derringer used short rayon, nylon, and glass fibers in natural rubber (NR) to increase the Young's modulus of the vulcanizates.<sup>1</sup> Moghe reported the milling parameters that cause fiber orientation and its influence on the composites' properties.<sup>2</sup> According to Coran et al.<sup>3</sup> the properties of cellulose fiber-elastomer composites depend on the type of elastomer used, fiber concentration, fiber aspect ratio, and fiber orientation. O'Connor compared the composites reinforced with five kinds of fibers and found that their mechanical properties depend on the type, volume loading, aspect ratio, orientation, and dispersion of fiber and fiber-matrix adhesion.<sup>4</sup> He also reported that for cellulosic fibers, a dicomponent dry bonding system consisting of hexamethylenetetramine (Hexa) and resorcinol is sufficient for getting good fiber-rubber adhesion, instead of the normal tricomponent dry bonding system consisting of hexa, resorcinol, and silica.

Though both synthetic and natural fibers have been used for reinforcing polymers, the natural fibers gained importance because of their low cost, availability, and good adhesion with the polymer matrix. De and co-workers have reported the results of their studies on short jute-fiber- and silk-fiber-reinforced NR, styrene butadiene rubber, and carboxylated nitrile rubber.<sup>5-8</sup> The use of coconut fiber as a reinforcing filler for NR has also been reported recently.<sup>9</sup> Nowadays, sisal fiber has gained wide importance as a reinforcing filler both for plastics and rubbers. Recently, Joseph et al.<sup>10,11</sup> reported on the mechanical properties of sisal-fiber-reinforced epoxy, phenol-formaldehyde, and thermoplastic composites. We have studied the mechanical properties of acetylated and untreated short sisal-fiber-reinforced natural rubber composites and found that acetylation improves the adhesion between the rubber and the fiber.<sup>12</sup>

The increasing use of short fiber composites in static and dynamic applications lead to the importance of stress relaxation measurements. Since the behavior of the rubber-fiber interface can be easily detected by stress relaxation studies. Vulcanized rubbers when subjected to constant deformation undergo a marked relaxation of stress both at low and high temperature.<sup>13</sup> The stress under a constant deformation decays by an amount substantially proportional to the logarithm of the period in the deformed state. The stress relaxation behavior of short jute fiber-nitrile rubber composites has been

\* To whom correspondence should be addressed.

studied in detail by Bhagawan et al.<sup>14</sup> They reported the existence of a two-stage relaxation pattern in these composites. Flink and Stenberg<sup>15</sup> studied the stress relaxation behavior of short cellulose fiber-natural rubber composites by using plots of  $E_{(t)}/E_{(t=0)}$  vs.  $\log t$ , where  $E_{(t)}$  is the stress at a given time and  $E_{(t=0)}$  is the initial stress. They reported that the stress relaxation measurement would give a clear idea about the level of adhesion in fiber-rubber composites. Stress relaxation behavior of short Kevlar-fiber-reinforced thermoplastic polyurethane has been reported by Kutty et al.<sup>16</sup> They reported a two-step relaxation mechanism for the unfilled stock and a three-stage relaxation process for the filled stock. In the present work we report the stress relaxation behavior of acetylated short sisal-fiber-reinforced natural rubber composites with special reference to the effects of strain level, fiber loading, bonding agent, and temperature.

## EXPERIMENTAL

### Materials

The sisal fiber obtained from Tamil Nadu, South India, is a lignocellulosic fiber, the reported chemical composition<sup>17</sup> and dimension of which is given in Table I. Natural rubber used for the study was ISNR-3 (light color) grade. The actual values of the specification parameters for the NR used in this study are given in Table II. Hexa and resorcinol were of laboratory reagent grade. All other ingredients used were of commercial grade.

### Chemical Treatment of Fiber

Sisal fiber was chopped to a length of 10 mm and was acetylated as per the methods reported by Chand et al.<sup>18</sup> The first step of acetylation was to immerse the fiber in 18% aqueous sodium hydroxide solution

Table II Properties of Natural Rubber

Dirt content, % by mass	0.03
Volatile matter, % by mass	0.50
Nitrogen, % by mass	0.30
Ash, % by mass	0.40
Initial plasticity, $P_0$	38
Plasticity retention index, PRI	78

at 35°C for 1 h. After this treatment, the fiber was washed with water several times and then dried. It was then soaked in glacial acetic acid for 1 h at 35°C, decanted, and then soaked in acetic anhydride containing two drops of concentrated sulfuric acid for 5 min. The fiber was filtered through a Buchner funnel, washed with water, and then dried in an oven at a temperature of 70°C for 24 h. The treated fiber was kept in polyethylene bags to prevent moisture absorption.

### Preparation and Molding of Compounds

Formulations of test mixes are given in Table III. The mixes were prepared in a two-roll laboratory model open mixing mill (152 × 330 mm) at a nip gap of 1.3 mm. The mixing time and the number of passes were maintained for all mixes. Orientation of the fiber in the mill grain direction was achieved by repeated passing of the uncured compound through a tight nip. Blanks cut from the uncured sheet were marked with the direction of the mill grain and were vulcanized at 150°C in a hydraulic press having steam-heated platens to their respective cure times, as obtained from Monsanto Rheometer. Test pieces were punched out from the molded sheet along and across the direction of fiber orientation. The orientations of fiber along and across the directions are shown in Figure 1. However, it is very difficult to get 100% orientation of the fiber in a particular direction. In the present case, it was found that about 90% of the fibers could be oriented in the desired direction by repeatedly passing the composite between the mill rolls under a tight nip.

The extent of fiber breakage in the compound was determined by dissolving the compound in benzene followed by extraction of fiber and examination of fiber length distribution using a polarizing microscope. The distribution of length of the extracted fibers is shown in Figure 2. Apart from reduction in length, there was no visible change in the straight cylindrical shape of the fibers due to the milling process undergone by the fibers.

Table I Characteristics of Sisal Fiber

Cellulose (%)	78
Hemicellulose (%)	10
Lignin (%)	8
Waxes (%)	2
Ash (%)	1
Diameter ( $\mu\text{m}$ )	100-300
Specific gravity	1.45

Table III Formulation of Mixes

Ingredients	A	B	C	D
Natural rubber	100	100	100	100
Zinc oxide	5	5	5	5
Stearic acid	1.5	1.5	1.5	1.5
Sisal fiber (acetylated)	—	10	15	15
Resorcinol	—	2.5	3.75	—
Hexa <sup>a</sup>	—	1.6	2.4	—
TDQ <sup>b</sup>	1	1	1	1
CBS <sup>c</sup>	0.6	0.6	0.6	0.6
Sulfur	2.5	2.5	2.5	2.5

<sup>a</sup> Hexamethylenetetramine.<sup>b</sup> 2 : 2 : 4-trimethyl-1,2-dihydroquinoline polymerized.<sup>c</sup> N-cyclohexyl-2-benzothiazyl sulfenamide.

### Stress Relaxation

The stress relaxation measurements were carried out in a Zwick universal testing machine, model 1474. The dimensions of the dumbbell-shaped test sample are given in Figure 3. The samples were pulled to a desired strain level at a strain rate of approximately  $0.061 \text{ s}^{-1}$  and the decay of stress as a function of time was recorded. The results presented here were obtained with samples cut from a single vulcanized sheet to minimize the experimental scatter.

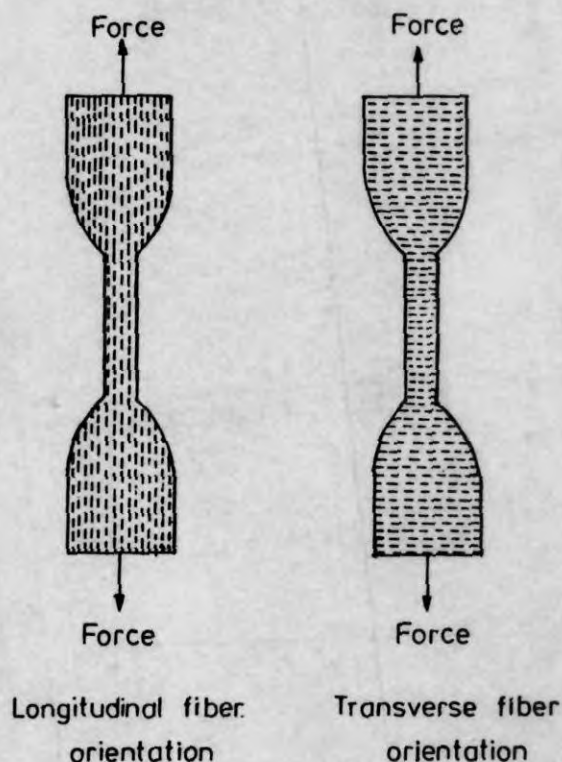


Figure 1 Longitudinal and transverse orientation of the fiber.

### RESULTS AND DISCUSSION

#### Fiber Breakage

Figure 2 gives the distribution of the length of the extracted fibers after mixing. It is seen that the initial 10 mm length of the fiber was reduced due to the high shear force generated during mixing, and a majority of the fibers (65%) have a length of 2–6 mm after mixing.

#### Stress-Strain Behavior

The stress-strain properties of the composites in longitudinal and transverse fiber orientations have been studied in detail.<sup>19</sup> The well-bonded, longitu-

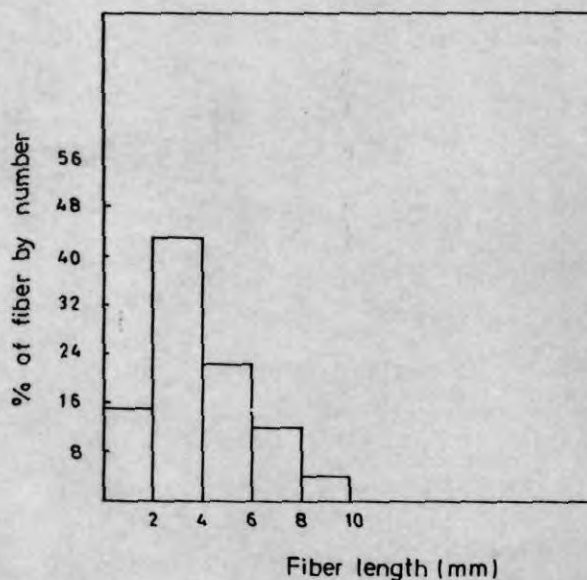
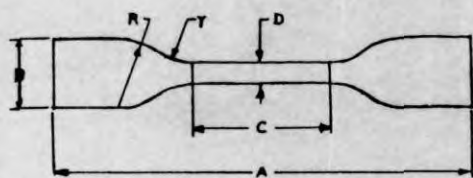


Figure 2 Distribution of fiber length after mixing.





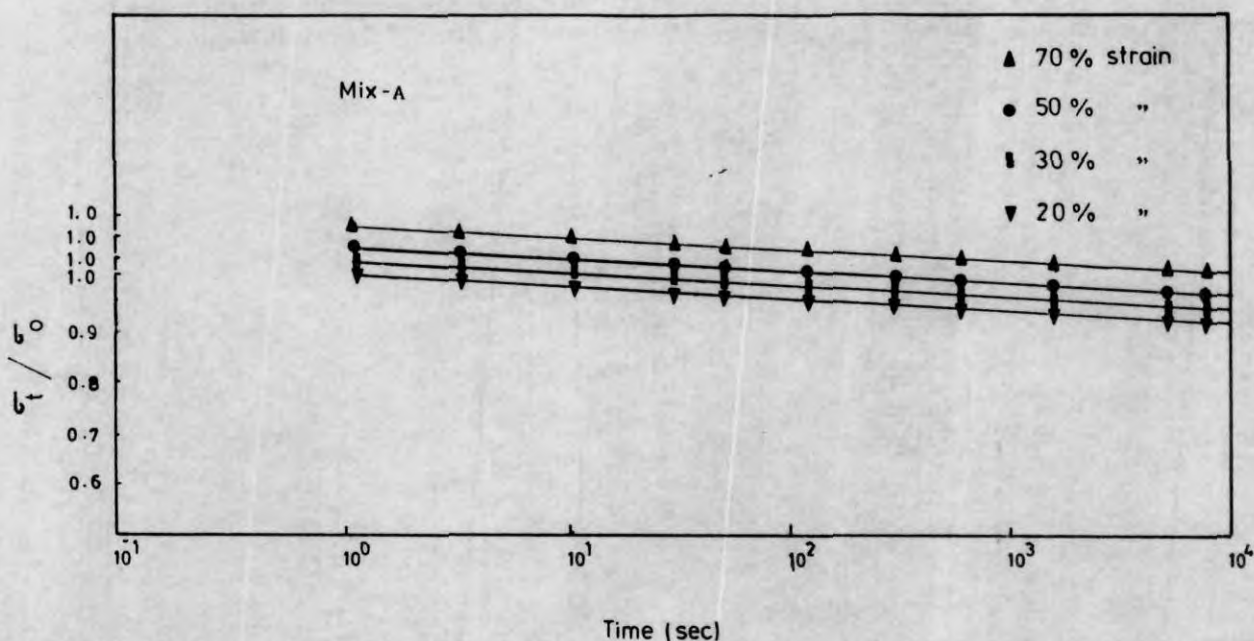
**Figure 3** Dimensions of the test specimen. Overall length (A): 115 mm; Width of ends (B): 25 mm; Length of narrow parallel portions (C): 33 mm; Width of narrow parallel portions (D): 6 mm; Small radius (r): 14 mm; Large radius (R): 25 mm; Thickness: 2 mm.

dinally oriented fibers impart very high modulus and provide low elongation ( $< 20\%$ ) for the composite. In the case of composites with no bonding agent, the modulus is lower and elongation is higher. This is due to weak fiber to rubber adhesion. Detailed mechanisms of failure of the composites, with and without bonding agent, have been reported by us in a recent publication.<sup>12</sup>

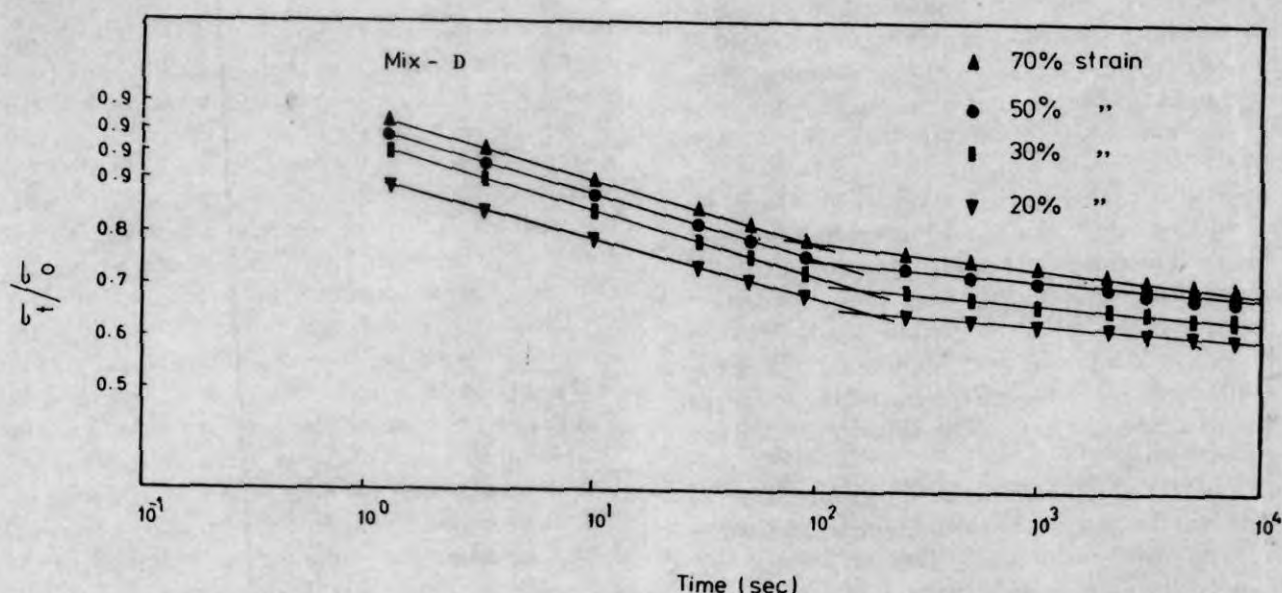
#### Effect of Strain Level (Longitudinal Fiber Orientation)

Figure 4 gives the stress relaxation plot,  $(\sigma_t/\sigma_0)$  vs.  $\log t$ , of the gum vulcanizate (mix A) at different strain levels. Where  $\sigma_t$  is the stress at a particular

time and  $\sigma_0$  is the stress at  $t = 0$ . The rate ( $0.061 \text{ s}^{-1}$ ) at which the initial strain attained is kept constant for all samples. It is seen that the experimental points for gum compound fall on a straight line, showing that the relaxation process involved only a single mechanism. There are two important mechanisms that can lead to stress relaxation in a cross-linked elastomer<sup>20</sup>: (1) physical stress relaxation due to molecular rearrangements requiring little primary bond formation or breakage and (2) chemical stress relaxation due to chain scission, crosslink scission, or crosslink formation. Under normal conditions, both physical and chemical stress relaxations will occur simultaneously. However, at typical ambient temperatures, the rate of chemical relaxation in a rubber like NR is very small, and the relaxation behavior is dominated by physical process except for very long periods. Here the relaxation patterns of the samples were studied at different elongation. However, it is interesting to note that the rates of stress relaxation at all the extensions studied are almost constant. According to Mackenzie and Scanlan,<sup>21</sup> the slope of stress relaxation plot of unfilled NR was independent of strain up to levels at which stress-induced crystallization occurs. It was also concluded that the mechanism is a physical one probably involving the protracted rearrangement of molecular chains or aggregates.<sup>13</sup> In the present case



**Figure 4** Stress relaxation curves of natural rubber gum (mix A). Successive graphs are displaced upward by 0.05 for clarity.



**Figure 5** Stress relaxation curves of mix *D*. Successive graphs are displaced upward by 0.05 for clarity.

also it is seen that the stress relaxation of the gum compound is independent of strain levels as indicated by almost parallel straight line plots (Fig. 4).

Unlike in the case of gum vulcanizates, the experimental points for the fiber-filled composites (containing longitudinally oriented fibers) fall on two intersecting straight lines (Figs. 5 and 6). The

stress relaxation curves consisting of two straight lines of unequal slopes indicate that a different mechanism of relaxation operates in the case of short fiber-filled composites: one that operates at shorter time ( $< 200$  s) and another that is prominent at the later stages of relaxation. It appears that a new relaxation mechanism operates in the fiber-filled

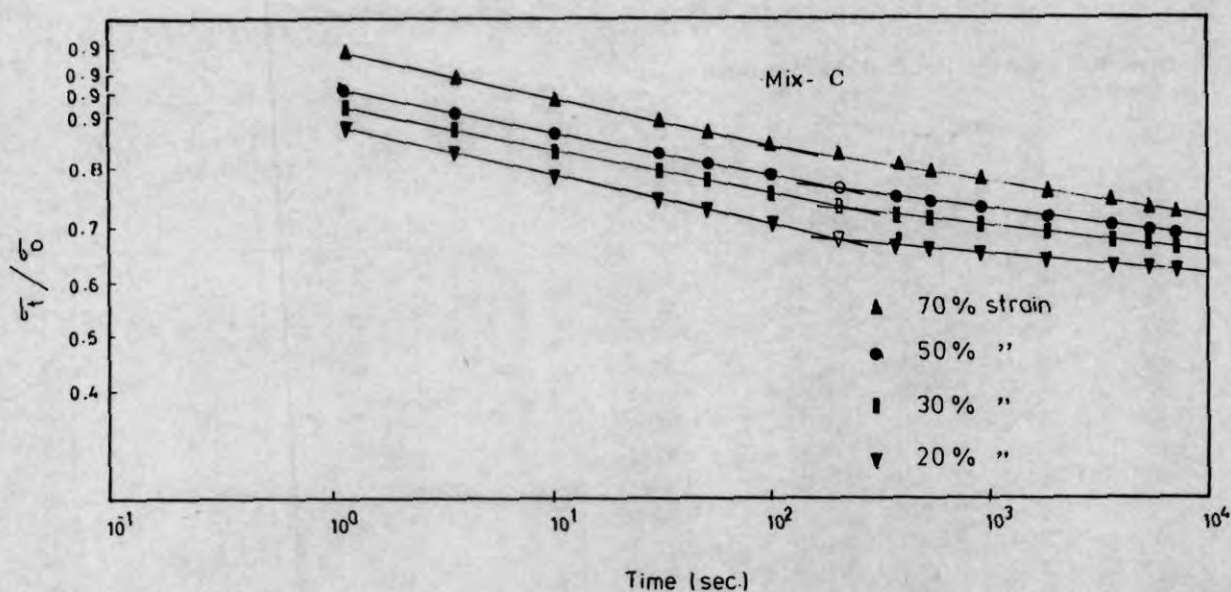


**Figure 6** Stress relaxation curves of mix *C*. Successive graphs are displaced upward by 0.05 for clarity.

composites and contribute significantly to the observed relaxation. It might arise from the progressive failure of rubber-fiber attachment either at the surface of the fiber or by rupture of the rubber molecules attached to them.<sup>13</sup> The point of intersection of these two straight lines is the time at which a change over from one mechanism to another takes place. The characteristics of the two mixes (control mix *A* and composite *D* with 15 phr acetylated fiber) can be realized from their slopes and intercepts given in Table IV. The slopes and intercepts were calculated using a linear regression method. The contribution by an earlier process of relaxation is calculated as reported by Mackenzie and Scanlan<sup>21</sup> by dividing the difference of the two intercepts by the intercept of the first line at  $t = 1$  s. The values obtained are given in Table IV.

In mix *D*, which contained 15 phr fiber loading and no bonding agent, the initial relaxation pattern increases with strain level. This is because the adhesion through weak bonds formed between treated fiber and rubber breaks as strain level is increased. In mix *C*, which contained 15 phr fiber loading and the bonding agent, the pattern of relaxation is the same as that in the case of mix *D*, but the initial relaxation rate remained almost constant with strain level. Due to good bonding, there is improved adhesion between fiber and rubber resulting in a strong interface. Therefore relaxation at the interface is not at all affected by low strain level. However, as in mix *D*, higher strain levels led to faster relaxation of stress in this case also. The second phase of relaxation, which is primarily due to the polymer, remains constant.

#### Effect of Bonding Agent (Longitudinal Fiber Orientation)

In Figure 7, the stress relaxation curves of *A*, *C*, and *D* at 30% elongation are presented. The gum compound *A* has the lowest rate of relaxation, and mix *D* has the highest rate of relaxation at 30% elongation (Table IV). We have seen earlier that the initial relaxation increases with strain level in a weak fiber-rubber interface, whereas it remains almost constant in a strong interface. By comparing the crossover time at same extensions of mix *D* and mix *C* (Table IV) we can have a clear idea about the level of adhesion between the fiber and the rubber in these two compounds. Mix *C* always registered a higher cross over time. This suggests that the initial relaxation is faster in a weak interface and hence a low crossover time for mix *D*. But in a strong interface as in mix *C*, the initial relaxation process is long and takes more time for the initiation of the second phase of the relaxation process.

From Table IV, it is seen that in the case of mix *D* the contribution of the early process changes from 21 to 7% as the strain level is varied from 20 to 70%. But in the case of mix *C*, which contained the bonding system, the contribution is nearly constant and independent of strain level.

#### Effect of Fiber Content (Longitudinal Fiber Orientation)

Figure 8 illustrates the effect of fiber loading (mix *A*, *B*, and *C*) which contained 0, 10, and 15 phr fiber, respectively, on stress relaxation at 50% strain

Table IV Results of Stress Relaxation Measurements

	Strain (%)	Slope (Negative)			Intercept			Contribution to Initial Mechanism (%)	Crossover Time (s)
		Early	Later	Difference	Early	Later	Difference		
Mix <i>A</i>	20	0.0427	—	—	0.9761				
	30	0.0481	—	—	0.9736				
	50	0.0500	—	—	0.9906				
	70	0.0520	—	—	0.9797				
Mix <i>C</i>	20	0.0834	0.0440	0.0394	0.8819	0.7353	0.0866	9.8	200
	30	0.0800	0.0450	0.0346	0.9115	0.8434	0.0681	7.5	180
	50	0.0848	0.0509	0.0339	0.9387	0.8848	0.0539	5.7	140
	70	0.0853	0.0809	0.0044	0.9600	0.8621	0.0960	9.9	120
Mix <i>D</i>	20	0.0854	0.0125	0.0729	0.9529	0.7532	0.1997	20.9	180
	30	0.0880	0.0109	0.0771	0.9243	0.7574	0.1669	18.1	160
	50	0.0892	0.0164	0.0576	0.9571	0.8083	0.1488	15.5	120
	70	0.0912	0.0196	0.0655	0.9270	0.8697	0.0573	6.9	91



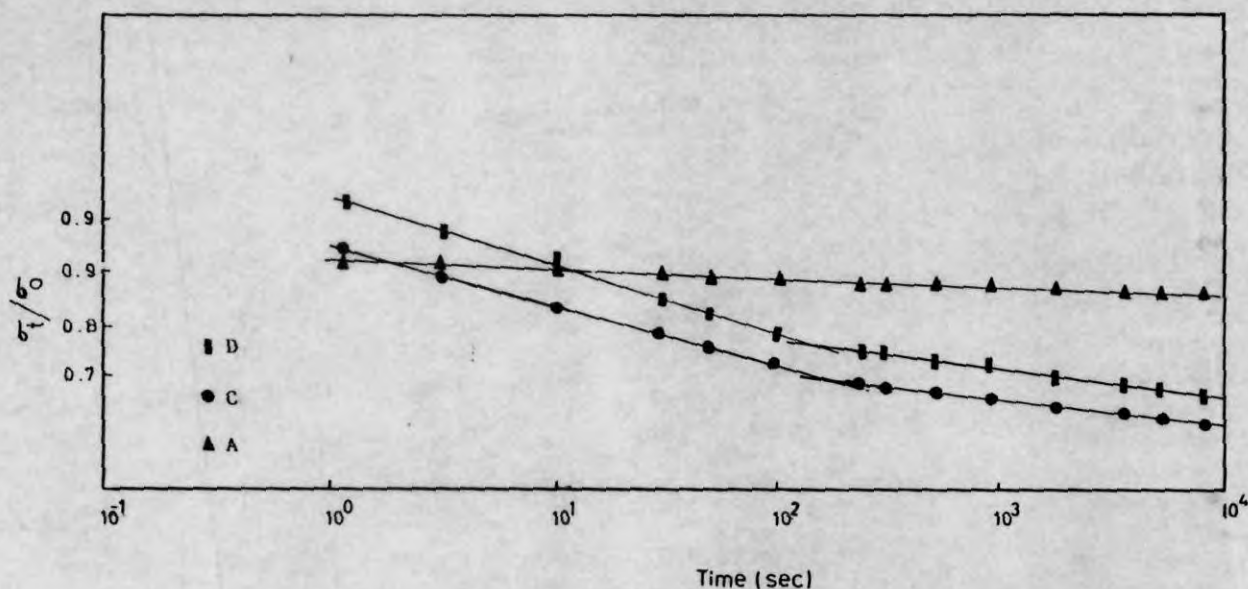


Figure 7 Stress relaxation curves of mixes A, C, and D at 30% elongation. The graph of mix D is displaced upward by 0.1.

level in the longitudinal fiber orientation. The rate of relaxation increases with fiber content, and also the time at which the earlier relaxation mechanism stops is shifted to higher value (Table V). According to the theory of strain amplification, owing to the inextensibility of the filler,<sup>22</sup> the strain in the elastomer matrix is greater than the overall strain, resulting in the rubber phase having an instantaneous modulus higher than for a gum rubber at equivalent extension. Derham<sup>23</sup> showed that the stress relax-

ation rate increases with carbon black loading. Similar results are obtained with short jute-fiber-filled NBR composites.<sup>14</sup> These findings are in agreement with our results.

The stress-strain relation of particulate-filled vulcanizates has been shown by Mullins and Tobin<sup>21</sup> in which substantially all of the observed extension is attributed to the deformation of "softened regions" with properties similar to those of the corresponding unfilled vulcanizate. The amount of ma-

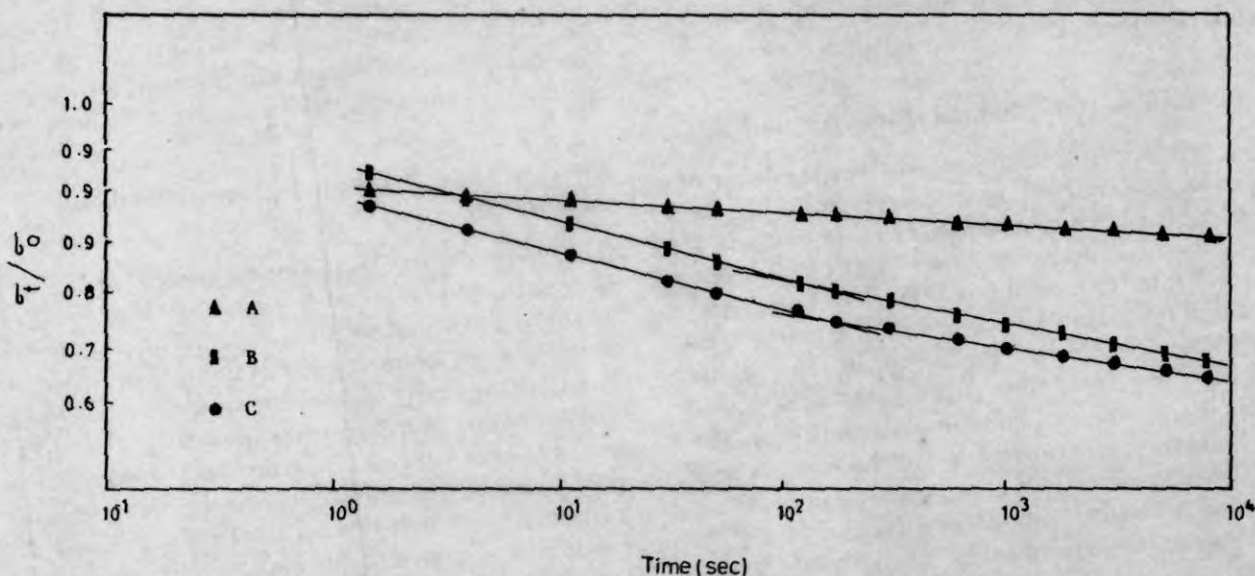


Figure 8 Stress relaxation curves of mixes A, B, and C at 50% elongation. Successive graphs are displaced upward by 0.1 for clarity.

Table V Effect of Fiber Concentration and Aging in Stress Relaxation Properties

	Strain (%)	Slope (Negative)			Intercept			Contribution to Initial Mechanism (%)	Crossover Time (s)
		Early	Late	Difference	Early	Late	Difference		
Effect of fiber content									
Mix A (no fiber)	50	0.0400	—	—	0.9906	—	—	—	—
Mix B (10 phr)	50	0.0792	0.0503	0.0288	0.9836	0.8346	0.149	15.1	120
Mix C (15 phr)	50	0.0848	0.0509	0.0339	0.9387	0.8848	0.053	5.6	140
Effect of aging									
Mix C	30	0.0833	0.0450	0.0393	0.8819	0.7953	0.086	—	200
Aging at 70°C for 4 days	30	0.0701	0.0394	0.0307	0.8224	0.7476	0.075	—	150
Aging at 100°C for 4 days	30	0.0397	0.0680	0.0280	0.7558	0.8130	0.057	—	50
Effect of aging									
Mix D	30	0.0880	0.0109	0.0771	0.9243	0.7532	0.199	20.8	160
Aging at 70°C for 4 days	30	0.0701	0.0178	0.0523	0.8220	0.6227	0.199	24.2	165
Aging at 100°C for 4 days	30	0.0518	0.0794	0.0276	0.8369	0.9949	0.158	—	199

terial in the softened state rises with imposed extension by a progressive breakdown of the original "rigid" structure. The fractional extension of the softened regions will be quite large, even when the imposed extension is small. Thus, even at small imposed extensions the regions taking part in the deformations are very highly strained. Relaxation of stresses would therefore be expected to proceed as in highly stretched unfilled rubber. The same mechanism is expected to take place in fiber-filled composites since here also the relaxation rate increases with strain level.

#### Effect of Aging (Longitudinal Fiber Orientation)

Aging produces interesting effects on the relaxation behavior of NR-sisal fiber composites (Fig. 9). Stress relaxation measurements have been made after aging the samples at 70 and 100°C for 4 days (Table V). In the case of mix D (no bonding agent), the initial relaxation rate decreased with aging. This may be due to the fact that some of the reactive groups in the treated fiber surface may be activated at high temperature to form bonds with rubber. The chemical stress relaxations due to chain scission or crosslink scission cause a sharp increase of the latter stages of relaxation rate of mix D aged at 100°C. The relaxation curve of mix C aged at 70°C regis-

tered the maximum crossover time and contribution to the initial relaxation. This is because the full strength of the bonding resin is developed during aging, which helps in obtaining better adhesion between the fiber and rubber, resulting in a strong interface. On the contrary the second-phase relaxation process of mix C aged at 100°C shows a sudden decrease in relaxation rate. There are two competing mechanisms leading to relaxation in the second stage: (1) chemical relaxation due to chain scission and (2) the bonding resin formation. Between these two competing processes, the degradation by molecular breakdown is the major factor.

#### Effect of Fiber Orientation (Longitudinal and Transverse)

The effect of fiber orientation on relaxation of stress is investigated for mixes D and C at 30% strain (Fig. 10). For the initial process, even in the presence of bonding agent, composites containing fibers oriented longitudinally have higher relaxation rate than those of composites with transverse fiber orientation (Table VI). In mix D it is observed that the slope of the initial rate of relaxation curve in the transverse direction is only half of that in the longitudinal direction. In transverse fiber orientation, the fibers are aligned perpendicular to the direction of force



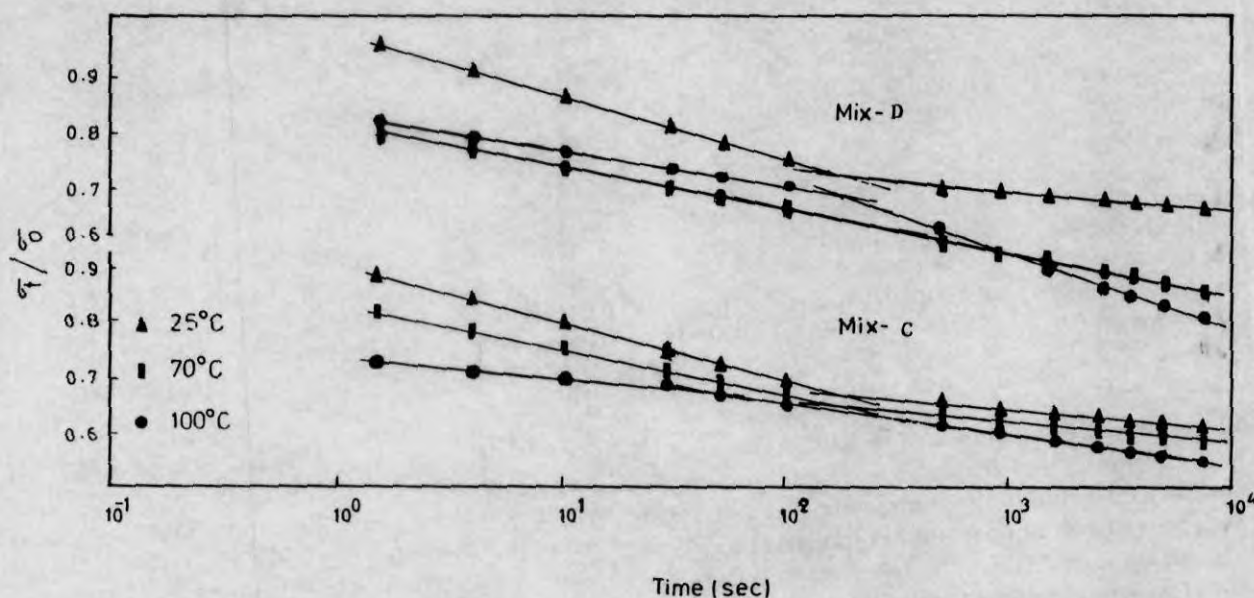


Figure 9 Stress relaxation curves of mixes *D* and *C* at 30% elongation (after aging).

application and the major relaxation is due to the polymer. In both the mixes the transversely oriented fiber composites have lower crossover time. In transverse fiber orientation, the fiber-rubber interface has a very small role in stress transfer and the initial relaxation process, which is entirely due to the fiber-rubber linkage, shifts quickly to the second relaxation process.

## CONCLUSION

A two-stage stress relaxation pattern was observed in acetylated sisal fiber-NR composites. The initial relaxation occurred at short times ( $< 200$  s), and the second-stage relaxation took much longer to complete the process. The initial mechanism is due to the fiber-rubber attachments and the latter one

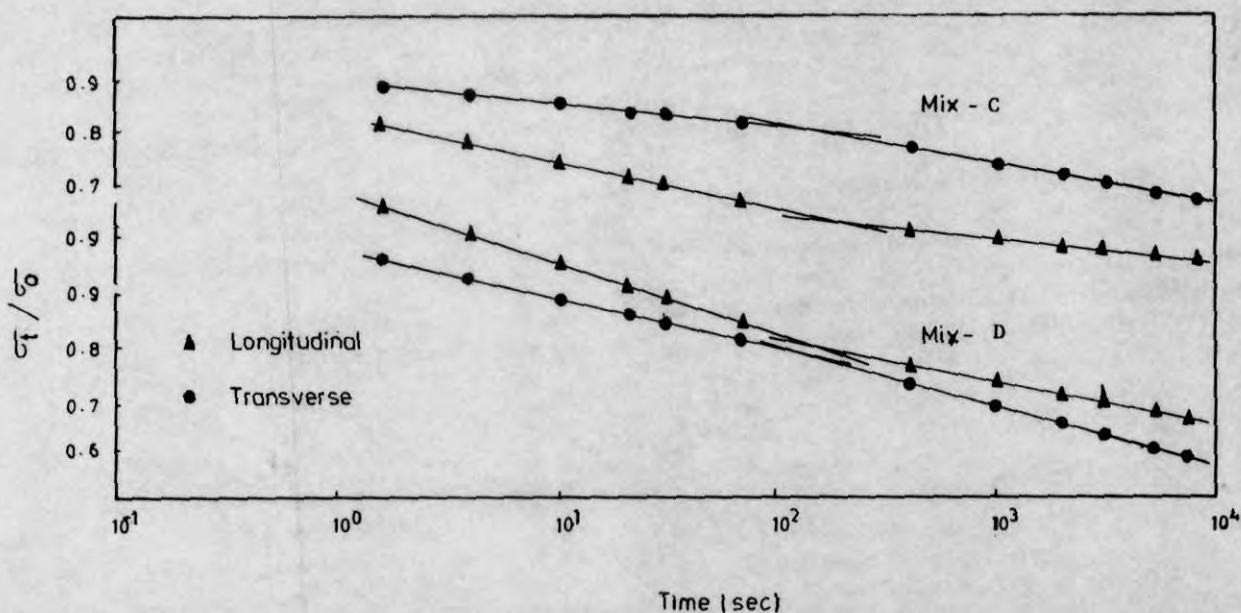


Figure 10 Stress relaxation curves of mixes *D* and *C* in the longitudinal and transverse direction at 30% elongation. The graph in the transverse direction of mix *D* is displaced upward by 0.1 for clarity.

Table VI Dependence of Stress Relaxation on Fiber Orientation

	Slope (Negative)		Difference	Intercept		Difference	Contribution to Initial Mechanism (%)	Crossover Time (s)
	Early	Later		Early	Later			
<i>Effect of fiber orientation</i>								
Mix C								
Longitudinal (30)	0.0800	0.0450	0.0346	0.9115	0.8434	0.0681	7.5	200
Transverse (30)	0.0640	0.0701	0.0011	0.9172	0.4882	0.0709	—	140
Mix D								
Longitudinal (30)	0.0880	0.0129	0.0771	0.9245	0.7374	0.1671	18.0	160
Transverse (30)	0.0405	0.0565	0.0160	0.9983	0.9912	0.0071	—	120

due to physical and chemical relaxation process of the natural rubber molecules. The relaxation process is influenced by bonding agent, which indicated that the process involved fiber-rubber interface. The gum vulcanizate showed only one relaxation pattern, the rate of which was almost independent of the strain level. For the composite in the absence of bonding agent, the rate of relaxation increased with strain level. But in the presence of bonding agent, the relaxation rate is almost independent of strain level because of the strong fiber-rubber interface. The initial rate of stress relaxation process diminished after aging.

## REFERENCES

1. D. C. Derringer, *Rubber World*, **45**, 165 (1971).
2. S. R. Moghe, *Rubber Chem. Technol.*, **49**, 1160 (1976).
3. A. Y. Coran, K. Boustany, and P. Hamed, *Rubber Chem. Technol.*, **47**, 396 (1974).
4. J. E. O'Connor, *Rubber Chem. Technol.*, **50**, 945 (1977).
5. V. M. Murty and S. K. De, *Rubber Chem. Technol.*, **55**, 287 (1982).
6. V. M. Murty and S. K. De, *J. Appl. Polym. Sci.*, **27**, 4611 (1982).
7. S. K. Chakraborty, D. K. Setua, and S. K. De, *Rubber Chem. Technol.*, **55**, 286 (1982).
8. D. K. Setua and S. K. De, *J. Mater. Sci.*, **19**, 983 (1984).
9. N. Arumugam, K. Tamareselvy, and K. Venkata Rao, *J. Appl. Polym. Sci.*, **37**, 2645 (1989).
10. K. Joseph, C. Pavithran, and S. Thomas, *J. Appl. Polym. Sci.*, **47**, 1731 (1993).
11. K. Joseph, C. Pavithran, and S. Thomas, *J. Appl. Polym. Sci.*, to appear.
12. S. Varghese, B. Kuriakose, and S. Thomas, *Indian J. Nat. Rubb. Res.*, **4**(1), 55 (1991).
13. A. N. Gent, *Rubber Chem. Technol.*, **36**, 697 (1963).
14. S. S. Bhagawan, D. K. Tripathy, and S. K. De, *J. Appl. Polym. Sci.*, **33**, 1623 (1987).
15. P. Flink and B. Stenberg, *Brit. Polym. J.*, **22**, 193 (1990).
16. S. K. N. Kutty and G. B. Nando, *J. Appl. Polym. Sci.*, **42**, 1835 (1991).
17. B. C. Barkakaty, *J. Appl. Polym. Sci.*, **20**, 2921 (1976).
18. N. Chand, S. Varma, and A. C. Khazanchi, *J. Mat. Sci. Lett.*, **8**, 1307 (1989).
19. S. Varghese, B. Kuriakose, S. Thomas, and A. T. Koshy, *Indian J. Nat. Rubb. Res.*, **5** (1 + 2), 18 (1992).
20. U. Meier and J. Kuster, *Rubber Chem. Technol.*, **57**, 254 (1984).
21. C. I. Machenzie and J. Scanlan, *Polymer*, **25**, 559 (1984).
22. L. Mullins and N. R. Tobin, *Proc. 3rd Rubber Technol. Conf. London*, 1954.
23. C. J. Derham, *J. Mater. Sci.*, **8**, 1023 (1973).

Received August 12, 1993

Accepted February 25, 1994